Journal of Coastal Research	22	3	547–560	West Palm Beach, Florida	May 2006

Inconsistent Grain Roundness and Sphericity Trends and the Valley Wall Influx Factor: Between Alpine Source and Lake Shore, SE France

Jean-Daniel Stanley and Victoria L. So

Geoarchaeology Program
E-206 NMNH
Smithsonian Institution
Washington, DC 20013-1712, U.S.A.
Stanley.daniel@nmnh.si.edu

ABSTRACT

STANLEY, J.-D. and SO, V.L., 2006. Inconsistent grain roundness and sphericity trends and the valley wall influx factor: between Alpine source and lake shore, SE France. *Journal of Coastal Research,* 22(3), 547–560. West Palm Beach (Florida), ISSN 0749-0208.

The greatest change in particle roundness, sphericity, and size in most fluvial systems generally occurs in the initial first few kilometers of sediment transport. Observations in natural settings and laboratory experiments have shown that changes, such as increased grain rounding and decreased size due to particle breakage, wear, and attrition, tend to be progressive along the dispersal path.

In marked contrast, this study records highly variable and poorly developed particle-texture trends downslope along short (<5 km) channels that extend directly from a high-relief carbonate source area down to the shore of Lake Annecy in the western Alps, SE France. The observed inconsistent patterns are measured in both a region-wide analysis using all collected samples and also in a more specific survey of samples in six different channels incised on the steep, topographically irregular mountain flanks that border the lake.

The major factor responsible for the irregular downslope patterns of roundness, sphericity, and size in the Annecy study area is the lateral introduction of sediment into the fluvial channels along dispersal paths. Episodic failure of mechanically unstable sediments and their transport down steep valley walls bring less-abraded sediment of variable shape and size along the dispersal paths. The valley wall sediment influx factor warrants further examination to better interpret sedimentation processes in dissected, high-gradient terrains that border coastal areas.

ADDITIONAL INDEX WORDS: *Abrasion, Alps, Annecy Lake, bedload, carbonate grains, fan-delta, lateral influx, proximal settings, sediment failure, texture, transport processes, valley wall sedimentation.*

INTRODUCTION

Measurements of sediment textures record the extent of wear, attrition, and other modifications to which sediment particles are subject during sediment transport. Textural attributes such as roundness, sphericity, and size are largely associated with events that occur during the dispersal process, when grains are abraded as a result of collision with each other and bedrock. Field observations and findings in controlled laboratory experiments have shown that grains tend to become progressively rounded, spherical, and smaller with transport distance. Roundness refers to the form of a grain as related to the sharpness or curvature of edges and corners, whereas sphericity is a measure of the degree to which a particle approximates the shape of a sphere. There is a large body of literature that pertains to change of such particle textures that occurs during transport as summarized by, among others, MARSHALL (1929), WADELL (1932), KRUMBEIN and PETTIJOHN (1938), KRUMBEIN (1941), CURRAY and GRIFFITHS (1955), PETTIJOHN (1957), KUENEN (1964), GRIFFITHS (1967), PETTIJOHN, POTTER, and SIEVER (1973), and FRIEDMAN and SANDERS (1978).

Investigations indicate that grain attributes are rapidly acquired within short travel distances during initial phases of sediment transport. Few studies, however, have focused specifically on the extent of changes in grain roundness, sphericity, and size that occur in natural settings at, or in close proximity to, source terrains. Results based on controlled laboratory experiments that use pebble-sized material modified in abrasion mills and tumbling barrels generally record rapid, yet fairly systematic, particle texture change within short distances. It is recognized that such laboratory results on coarser materials do not necessarily closely apply to associated finer-grained granule and sand-sized materials, nor do they exclusively replicate conditions in fluvial and other natural settings (PETTIJOHN, 1957).

The present investigation examines downslope trends of roundness, sphericity, and grain size in a natural setting comprising six streams incised in high-relief carbonate terrains of the western Alps in SE France (Figure 1). Fluvial torrent and stream channels of diverse configuration in this proximal sector receive seasonally variable flow and are characterized by generally steep axes. The study area was select-

DOI:10.2112/05A-0022.1 received and accepted 13 July 2205.

Financial support for the study was provided by a Walcott Fund award (NMNH), Smithsonian Institution, Washington, D.C.

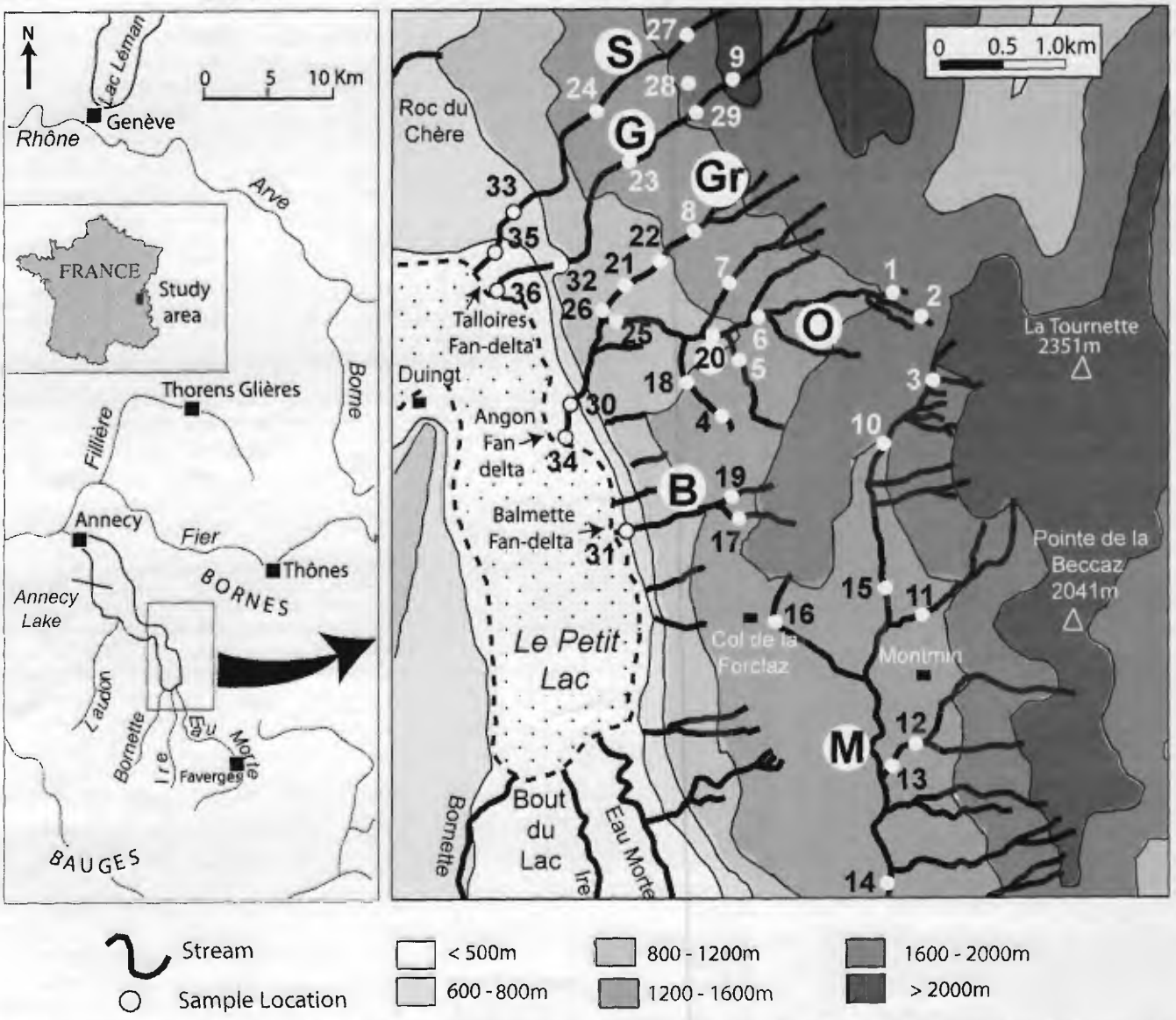

Figure 1. Maps of Annecy Lake study area in SE France (insets) and the region east of Le Petit Lac. Shown are 36 localities (white dots), steep *nant* channels (S = Sec, G = Graz, Gr = Grenant, O = d'Oy, B = Balmette, M = Montmin), fan-deltas on lake shore, elevated carbonate ridges (including La Tournette), and population centers.

ed primarily on the basis of four criteria: (1) short distance (<5 km) and rapid change in relief (>1000 m) between the high source terrains and lake margin at much lower elevation; (2) channel axes confined by adjacent, steep valley walls; (3) sediment supply comprising a wide range of grain size; and (4) availability of a dominant particle lithology (>90% carbonate) that affords consistent comparisons of textural changes along the dispersal paths (*i.e.*, roundness, sphericity, and size attributes are closely associated with composition). Of particular interest here is the nature of downslope textural changes in bedload sediment along the initial several kilometers of transport in short, steep channels in steep, rugged terrains between cliffs and the shore of Lake Annecy below. The downslope evolution of grain parameters in different size fractions is examined in a region-wide study and, more specifically, along six distinct channel dispersal paths.

GEOGRAPHIC AND GEOLOGIC FRAMEWORK

Lake Annecy (L.A.), positioned south of the city of Annecy in the Haute Savoie, is an ice-carved depression formed between the Bauges and Bornes mountain chains (NICOUD and MANALT, 2001). The lake surface is at an elevation of 446.5 m above mean sea level (msl) and covers an area of 27 km^2. This 14.6-km-long lake is subdivided by a submerged ridge at Duingt into the smaller NNW-SSE–oriented sector named

Petit Lac and the larger NW-SE–oriented Grand Lac, with the city of Annecy at its northern shore (Figure 1). The Grand Lac at its widest exceeds 3 km; the maximum depth of the Petit Lac is ~55 m and that of the Grand Lac is ~67 m. The L.A. drainage basin area is 251 km². Four rivers of modest size—the Laudon, Eau Morte, Ire, and Bornette rivers (Figure 1, inset)—flow during most of the year to the southern and southwestern lake margins and account for ~75% of total discharge (STANLEY and JORSTAD, 2004); to the north, lake water drains into the Fier River at Annecy. Numerous other fluvial channels, mostly small torrents and streams (many seasonally dry), account for the remaining 25% discharge to the lake margins. Currently, the population density is concentrated within 2 km of the lake margin; modest to sparse populations in villages and individual farms are found in the higher-elevated areas on mountain flanks.

The study area, covering an area of ~48 km², is positioned in the Bornes chain between the Petit Lac and several N-S–trending, high-relief ridges to the east (Figure 1). The highest elevation (2351 m) is at La Tournette, 4.2 km east of the lakeshore (Figure 2A); other major relief features include the Pointe de la Bajulaz, 2254 m; Rochers du Varo, 2176 m; Pointe de la Beccaz, 2041 m; and Dents de Lanfon, 1824 m (INSTITUT GEOGRAPHIQUE NATIONAL, 2003). These high ridges are characterized by near-vertical cliffs that drop to elevations of ~1600 m above msl (Figures 2A and 2B). At their uppermost reaches, some fluvial systems in this sector (locally named *nants*) begin as narrow channels that cascade down from high ridges as small waterfalls (Figure 2C); others begin as incised channels below the ridge cliffs and then descend 1200 m or more down to the lake margin. The western-sloping mountain flanks between the base of ridge cliffs and the lakeshore ranges from 3.0 to 4.4 km in length, and their slopes average from 17° to 25°. Locally, channel walls are of high relief (to >300 m) and steep (to >40°). The axial profile of channels below the ridges are step-like with slopes ranging from <10° to vertical, such as the Nant d'Oy at its high waterfall at the Cascade d'Angon (just below sample sites 25 and 26; Figure 1). Lengths of stream channels to the lake shore range from 1.9 to 5.1 km.

Four of the six fluvial systems examined in the study area terminate on fan-deltas formed at the eastern shore of the Petit Lac. These are, from north to south: the Nant Graz and Nant Sec at Talloires (Figure 3A); the Nant d'Oy at Angon (Figures 3A and 3B); and Nant Balmette at Balmettes (Figure 2B). High-flow stages and periodic floods in these fluvial systems usually result from two events: winter–spring snow melt and summer–autumn rainstorms. This flow is for the most part confined within high-relief depressions by steep-walled rock (carbonate, marl) exposures and scree deposits (Figures 2E and 2F) and funneled to lower elevations where valleys open and relief decreases markedly near the lake margin. Channels, at the base of the slope and on fan-delta surfaces along the Petit Lac, are artificially maintained by walls and levees for flood control (Figure 4F). Nevertheless, at times of high discharge, sediment reaches the mouths of streams at the lake shore (Figures 3C and 3D).

The study area lies within the tectonically-deformed sector of the western Alps that include primarily Mesozoic limestone, dolomitic limestone, and marl (DOUDOUX *et al.*, 1992). The sector east of the lake is characterized by structurally displaced sedimentary units dominated by massive, well-exposed, limestone strata of Cretaceous (Urgonian) age (Figures 2A–2C) topped locally by younger (Maastrichtian) lithographic limestone. High crests formed by these units are oriented from N 20°W to N 25°E. The Cretaceous formations lie above Jurassic units comprised of lithographic limestone and alternating limestone and marl beds of Kimmeridgian and Oxfordian age; these older strata are partially exposed along midslope sectors (Figures 2A, 2B, and 3A) and locally on the Petit Lac margin. The Mesozoic units are offset by faults, some of which have been active during the Holocene.

The geologically much younger Quaternary cover is irregularly distributed across this area and comprises mostly carbonate debris of fine to coarse size (boulders to >6 m diameter) deposited during the late Pleistocene; this includes Würmian tills, fluvioglacial and lacustrine deposits, and slope scree. Formation of L.A. has been created by major glacial erosional and depositional events in the Pleistocene (DOUDOUX *et al.*, 1992; OLDFIELD and BERTHIER, 2001). A subglacial lake began to develop about 16,600 years ago, and L.A. gradually evolved from a glacial to biologically productive lacustrine system by ~14,000 years ago. Most Holocene to modern sediment displaced in torrent and stream channels east of the Petit Lac is formed of clastic debris from Mesozoic and Quaternary carbonate-rich source areas. The nature of downslope textural changes of fluvially transported particles between high Alpine and lake shore settings is the focus of the present study.

METHODOLOGY

A total of 36 samples were collected in the study area (Figure 1), and of these, 28 were recovered along the axes of six stream-channel paths. They are identified as follows, from north to south: Nant Sec, Nant Graz (Figure 4F), Nant Grenant (Figure 4D), Nant d'Oy (Figures 2E, 2F, 3A, 4A, and 4C), Nant Balmette (Figure 2B), and Nant Montmin (Figures 2C and 4B). The first five flow toward the west, whereas the Montmin flows to the south. An additional eight samples (at sites 4, 5, 7, 11, 12, 16, 18, and 28) were collected at midslope in minor depressions other than the six fluvial systems listed above. Approximately 350 g of surficial clay to pebble-sized sediment was recovered in the uppermost 2 cm of streambed deposits. The aim was to collect material recently displaced (during the past decade) by seasonally variable, but at times significant, snowmelt and rainfall.

A splitter was used to obtain a representative cut from each sample, and this selected material was then wet-sieved and oven-dried. Most sediment cuts included sufficient material to measure at least 300 grains in the 1.19- to 2.0-mm (coarse sand) and 2.0- to 4.76-mm (granule) fractions; however, some samples contained a smaller number (usually <150 grains) of particles for measurement in the 4.76- to 6.35-mm (small pebble) fraction. For purposes of this study, these three fractions are referred to as fine, medium, and coarse (coded, respectively, Fi, Me, and Cse; Table 1).

Samples were examined in a random (blind) sequence to

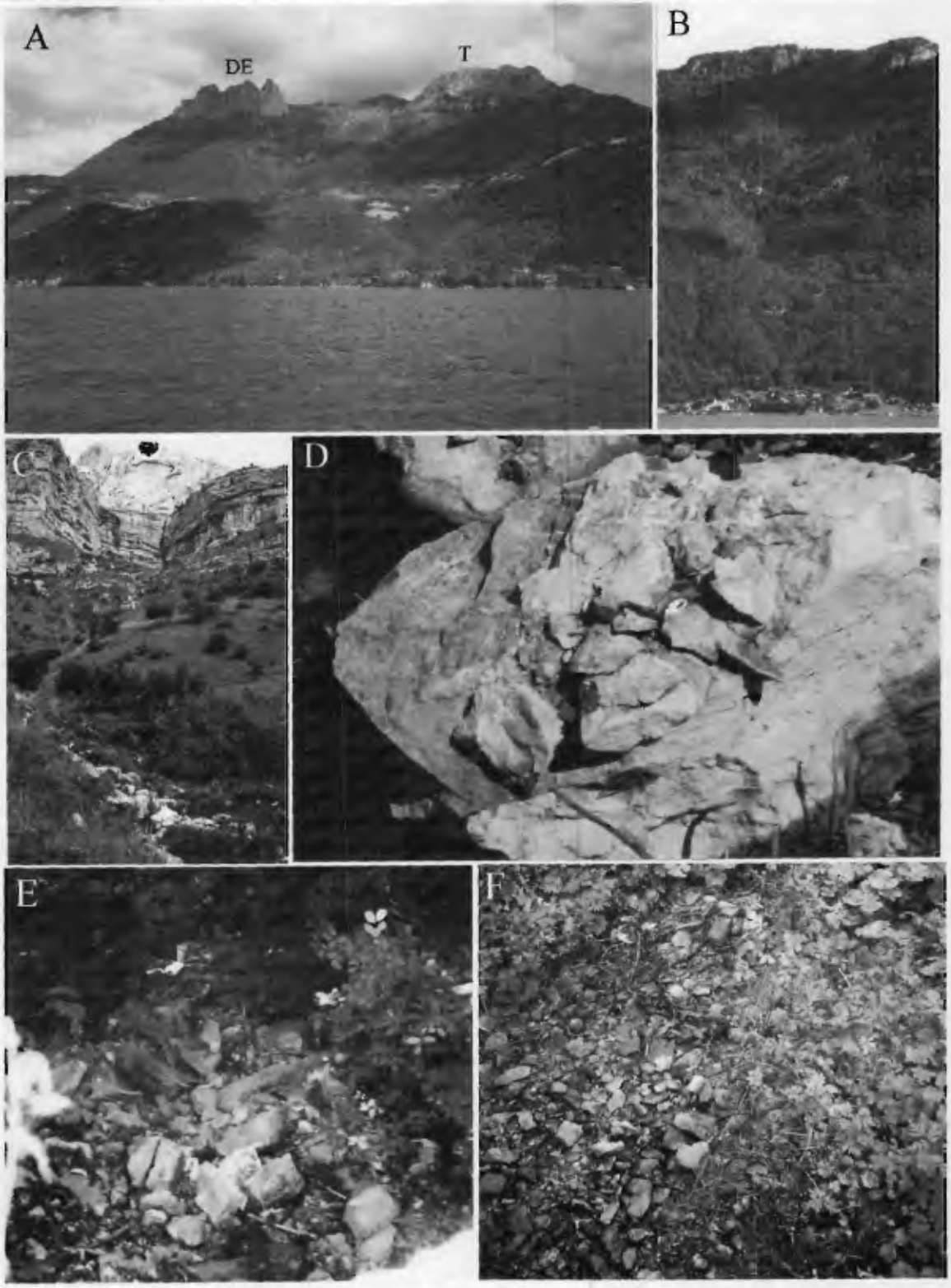

Figure 2. Photographs of the Annecy Lake study area: (A) high Cretaceous limestone ridges, including Dent de Lanfon (DE) and La Tournette (T), and midslope Jurassic limestone exposures on the eastern margin of Petit Lac; (B) Nant Balmette and its fan-delta along Petit Lac; (C) La Tournette ridge with small waterfall and upper Nant Montmin channel with its boulders and coarse sediment fill (near sample site 3); (D) weathered exposure of laminated Cretaceous limestone at La Tournette ridge (near site 2); (E) angular and flat debris of variable size in Nant d'Oy (site 2); and (F) scree at base of valley wall on midslope near Nant d'Oy (sample site 6). **For color version of this figure, see page 595.**

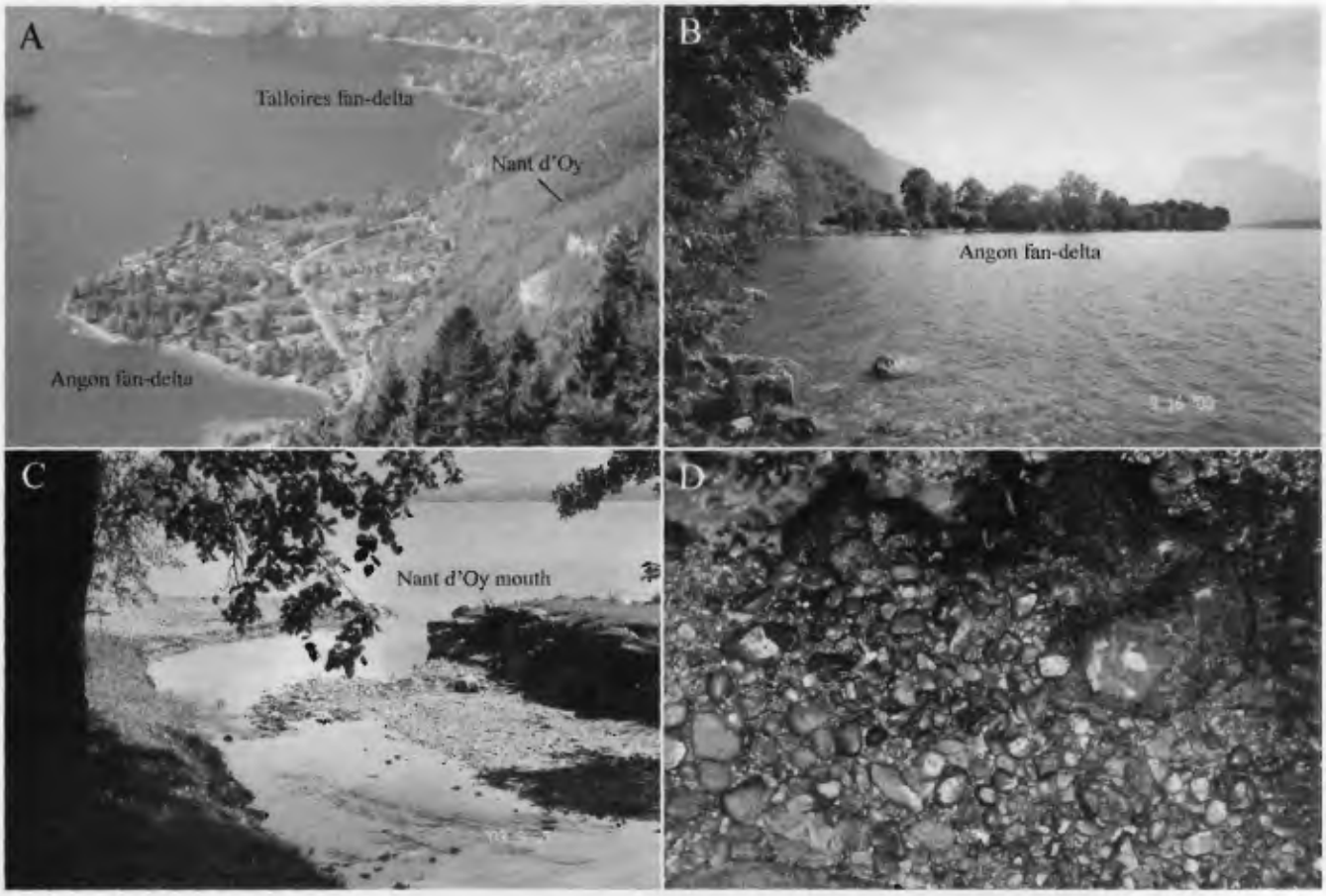

Figure 3. Photographs of Petit Lac margin: (A) Talloires (in distance) and Angon fan-deltas; note Nant d'Oy channel extending to Angon fan-delta and Jurassic limestone exposures on midslope; (B) Angon fan-delta extending into the lake; (C) mouth of the Nant d'Oy at Angon fan-delta coast; (D) subrounded and rounded carbonate pebbles and cobbles of diverse sphericity in the Nant d'Oy at the Angon fan-delta coast (leaf at lower left, 6-cm-long, provides scale). **For color version of this figure, see page 596.**

minimize locality bias when making textural measurements. Sphericity and roundness were visually evaluated by a single operator (second author) using a stereoscopic microscope to measure each grain on a numbered grid plate. For each of the three grain sizes in a sample, ~300 grains were separated into four sphericity classes (coded I–IV) using the Zingg classification (Figure 5, lower): I, tabular; II, equant; III, bladed; and IV, prolate. The roundness of each grain in these four sphericity categories was then determined. Each grain was initially assigned to one of five roundness classes (coded A–E): A, angular; B, subangular; C, subrounded; D, rounded; and E, well-rounded (Figure 5, upper; after PETTIJOHN, 1957). A total of 28,679 grains were counted in the 36 samples, accounting for an average total of ~797 grains examined in each sample. Particles in the three size fractions (Fi, Me, and Cse) were physically separated into four sphericity (I–IV) and five roundness (A–E) classes (Figure 6). Comprehensive tabulated numerical and percentage listings for all the above data are available from the authors.

In addition, two grain size analyses (original and replicate grain-size run) for each of the 36 samples were performed using a Coulter Counter LS200 laser particle analyzer (Beckman Coulter, Fullterton, California). The following grain-size parameters were determined for each sample: % sand (63–2000 μm), % silt (0.5–63 μm), and % clay (<0.5 μm); mean, median, and modal grain size; and standard deviation (SD). The original and replicate grain-size data for the two cuts in each sample were then averaged for use in this study (see Table 2). Sediment in most samples includes large proportions of sand and silt, with lower amounts of pebbles, granules, and clay. There are 15 sand (>75% sand fraction), 17 silty sand (50–75% sand fraction), and four sandy silt (<50% sand fraction) samples.

Significant parameters of roundness, sphericity, and grain size for the three main size fractions (Fi, Me, Cse) in each sample were tabulated into a database. This information was then was statistically and graphically compiled (scatter plot diagrams) using Microsoft Excel (Figures 7–12); included in this database are linear regression trend-lines and R-squared (R^2) values.

(1) Initially, a regional all-inclusive comparison was made of roundness and sphericity data using all 36 samples. The

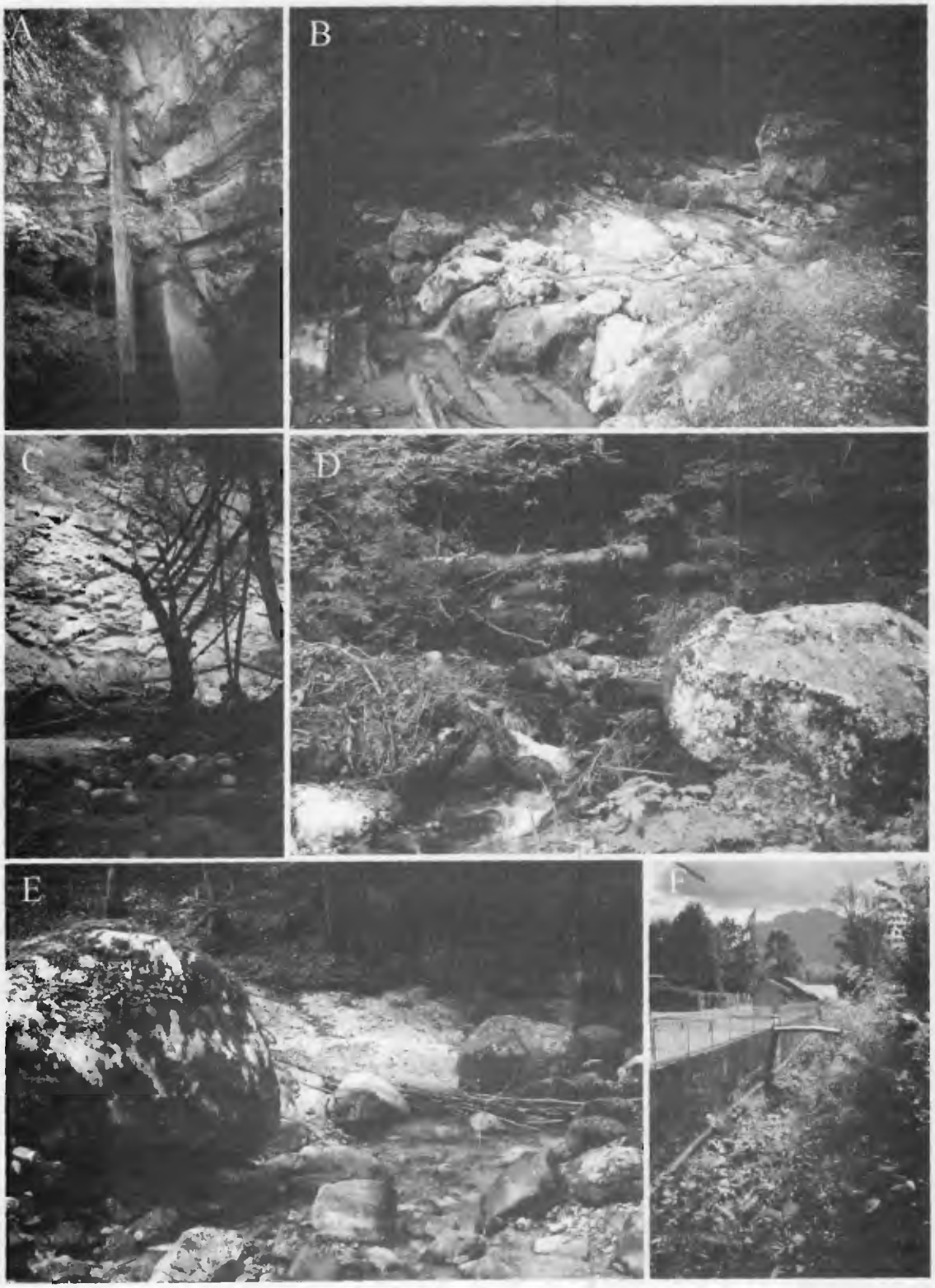

Figure 4. Photographs of selected sites in the study area: (A) Nant d'Oy (below site 25) at Cascade d'Angon (Jurassic limestone); (B) small branch at site 11 above Nant Montmin, flowing across exposures of Jurassic limestone at midslope; (C) Jurassic limestone forming valley wall at sample site 25; (D) boulders (diameter to 3.5 m) along Nant Grenant, at midslope near site 8; (E) large boulders (to 4 m) at site 25; and (F) Nant Graz near site 36, artificially channelized in town of Talloires. **For color version of this figure, see page 597.**

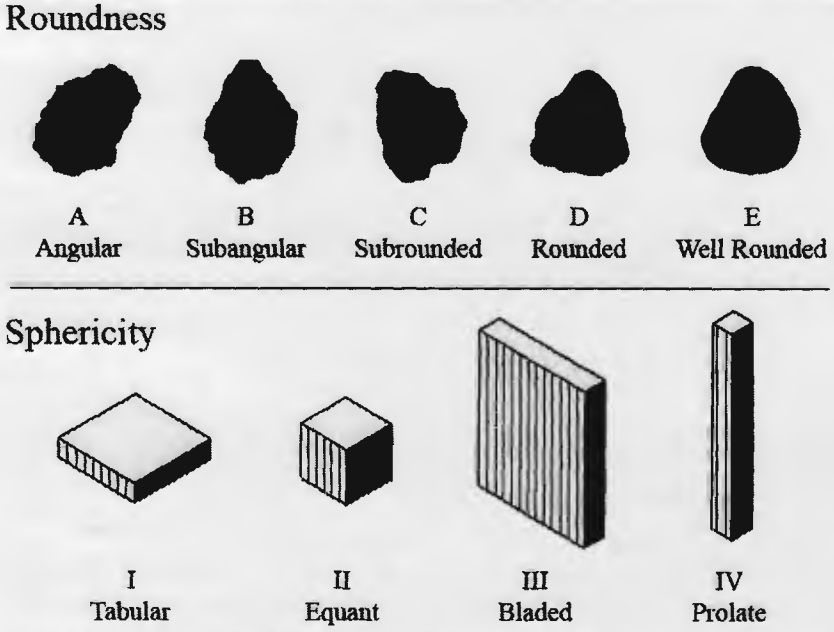

Figure 5. Classifications used in study (after PETTIJOHN, 1957): (upper) roundness classes A–E, and (lower) sphericity classes I–IV.

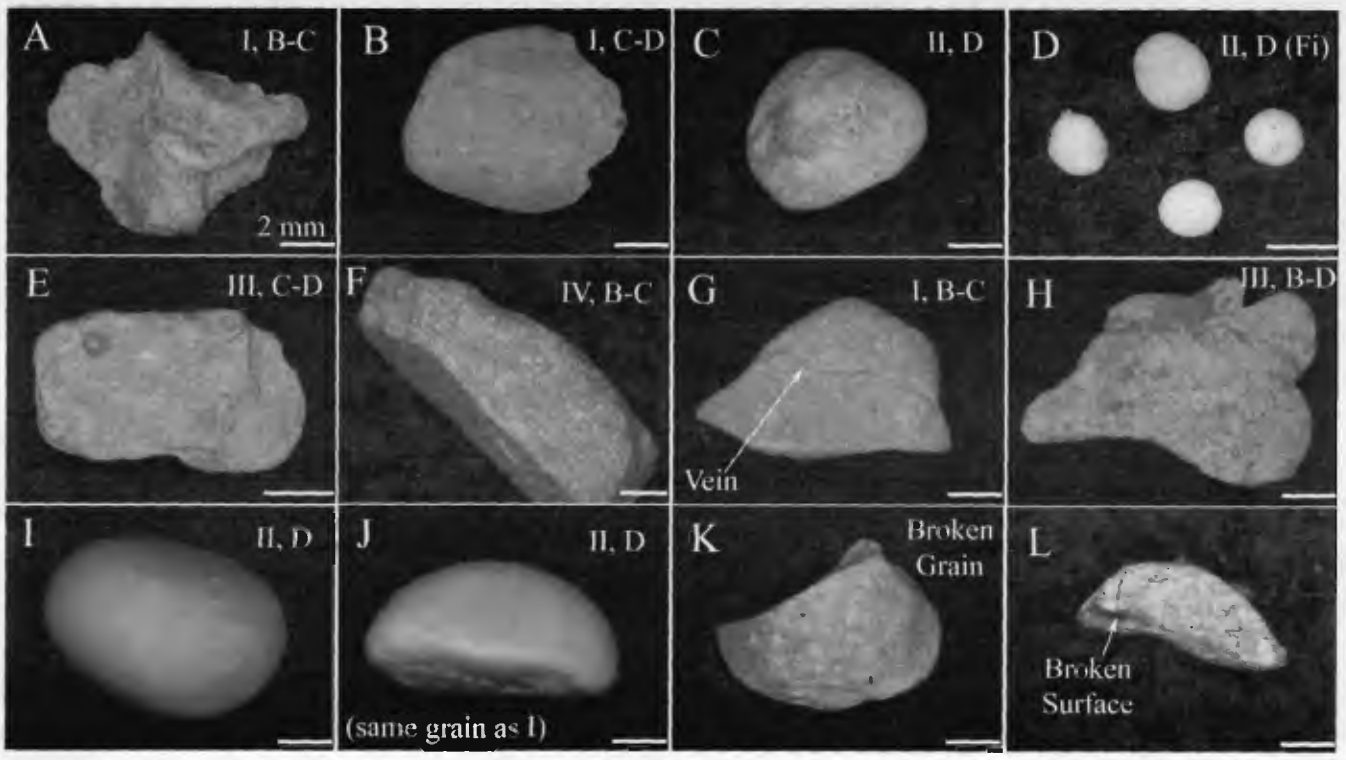

Figure 6. Selected limestone grains from study area; all particles are of coarse (Cse) fraction, except D, of fine (Fi) fraction. Roundness and sphericity identifications in upper right corner; vein is shown in G; fractured particles in I–L; white bar scale = 2 mm. **For color version of this figure, see page 598.**

Table 1. *Percentages of particle roundness (A–E) and sphericity (I–IV) in fine (Fi), medium (Me), and coarse (Cse) size fractions examined in study area. Calculated averages values are listed.*

	Roundness (%)				
	A	B	C	D	E
Fi	0.4	10.5	60.4	28.1	0.6
Me	0.6	11.7	51.0	36.1	0.6
Cse	1.8	17.3	46.6	32.5	1.8
Average	0.6	11.8	54.9	31.9	0.7
	Sphericity (%)				
	I	II	III	IV	
Fi	33.6	38.4	18.2	9.8	
Me	41.4	29.6	21.1	7.9	
Cse	35.1	29.4	29.4	1.0	
Average	37.0	33.7	20.7	8.6	

Fi = fine, Me = medium, Cse = coarse.

five roundness classes were compared among each other as were the four sphericity classes. Region-wide data pertaining to sand and silt percentages as well as mean grain size were also evaluated. From this survey base, graphs that revealed statistically indicative trends were selected for further analyses. On this basis, the less-frequently occurring roundness classes A and E (<0.7% of total) and sphericity class IV (<8.6% of total) were excluded from the database.

(2) Region-wide patterns of roundness (B, C, D) *vs.* sphericity (I, II, III) were then compared using all 36 samples. From results obtained, three textural classes (B, D, II) that appeared to be most useful were selected, and these were evaluated against specifically chosen grain size data (percent sand, mean size) that showed trends for the region as a whole.

(3) Graphs were also generated to detect any possible region-wide influence of dispersal distance along channel downslope from the source *vs.* sphericity and roundness, for the fine (Fi), medium (Me), and coarse (Cse) particle fractions. These parameters were further tested using the distance from the source area and the elevation above mean sea level of a sample *vs.* grain size (percent sand and silt, mean size). These relationships were examined region-wide using all 36 samples.

(4) A comparison was made using only seven samples collected at extreme proximal and distal geographic positions in

Table 2. *Elevation, distance from source, and grain-size parameters for 36 samples collected in the Lake Annecy study area (sample sites shown in Figure 1).*

Annecy Sample ID	Elevation (m)	Distance from Source (km)	% Sand	% Silt	% Clay	Mean (μm)	Mode (μm)	SD (μm)
1	1300	0.45	91.57	6.78	1.65	705.1	1443.0	503.9
2	1360	0.25	85.95	11.99	2.06	647.2	1443.0	510.7
3	1380	0.4	74.78	21.59	3.63	461.2	1584.0	493.1
4	940	0.9	88.14	9.77	2.09	562.1	1197.0	485.2
5	880	0.9	83.68	13.55	2.77	509.2	1091.0	478.0
6	900	1.65	85.75	10.4	3.85	653.9	824.5	433.6
7	920	1.1	57.73	29.41	12.86	189.3	269.2	231.7
8	910	1.0	47.38	39.45	13.17	193.9	429.2	260.1
9	880	1.35	61.17	28.8	10.03	226.4	390.9	261.9
10	1216	0.11	52.37	34.91	12.71	161.7	245.2	231.0
11	1040	1.6	87.63	8.05	4.32	591.3	905.1	424.6
12	1000	2.0	92.71	5.37	1.92	830.2	1197.0	478.1
13	879	3.71	95.12	3.64	1.24	826.3	993.6	447.7
14	809	4.51	90.34	7.72	1.94	731.9	1443.0	525.3
15	1006	1.81	95.53	5.17	1.30	897.5	1443.0	498.7
16	1104	0.8	70.11	24.86	5.03	504.1	1197.0	532.1
17	1052	0.55	74.40	20.05	5.55	490.8	905.1	455.2
18	850	1.25	34.22	53.24	12.54	115.7	34.58	189.9
19	1030	0.75	71.06	24.11	4.83	362.4	356.1	397.1
20	776	2.5	71.07	22.10	6.83	380.6	905.1	421.5
21	750	1.95	71.94	23.02	5.04	232.5	168.9	277.2
22	820	1.35	62.96	29.82	7.22	394.7	905.1	445.2
23	695	2.2	33.44	53.21	13.35	112.0	28.7	190.6
24	710	1.9	58.06	31.89	10.05	249.5	429.2	295.1
25	680	3.5	62.90	28.09	9.01	180.4	223.4	202.9
26	740	2.35	89.67	8.59	1.74	683.3	993.6	484.3
27	960	0.9	84.68	13.11	2.21	540.9	993.6	481.2
28	850	1.35	72.67	23.02	4.31	394.0	390.9	413.5
29	820	1.75	83.08	13.06	3.86	587.1	1314.0	510.1
30	455	3.5, 4.7	95.67	3.55	0.78	962.8	1584.0	503.7
31	480	1.85	48.61	42.21	9.18	191.2	45.75	272.2
32	500	2.9	70.67	23.70	5.63	385.5	517.2	416.5
33	490	2.6	71.86	24.39	3.75	325.9	245.2	381.9
34	450	3.85, 5.1	77.70	17.34	4.96	695.0	1197.0	536.1
35	460	3.1	65.33	29.62	5.05	263.7	356.1	308.1
36	450	3.35	66.13	28.32	5.55	307.8	471.1	342.7

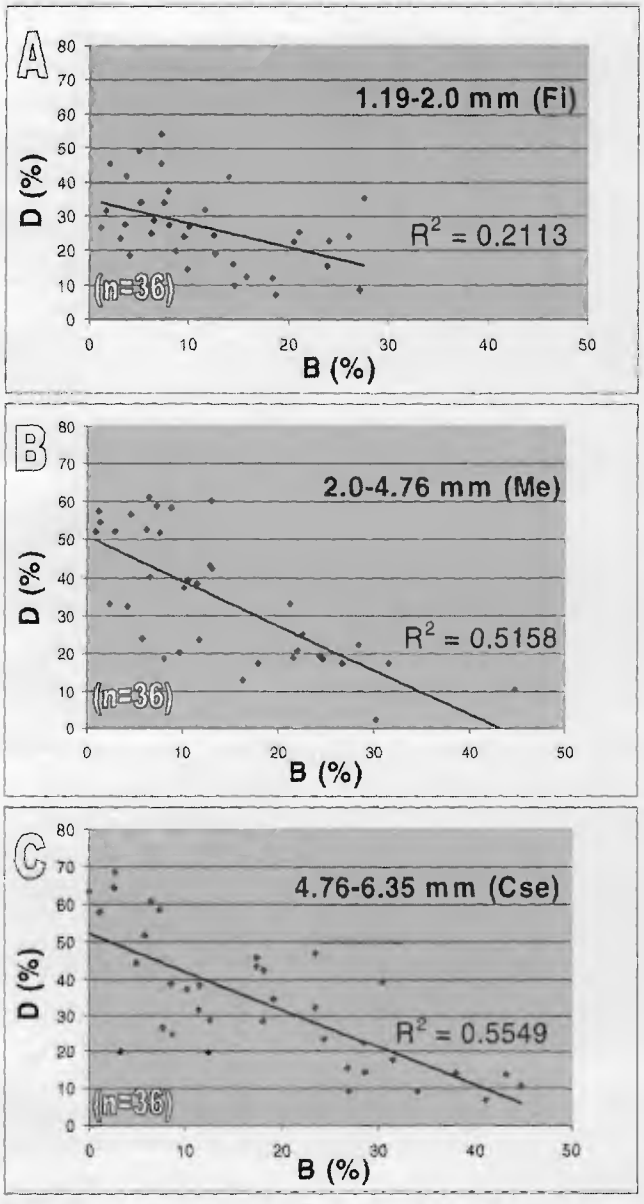

Figure 7. Scatter plots (region-wide, all samples, n = 36) showing inverse relationship between subangular (B) and rounded (D) classes in (A) fine, Fi; (B) medium, Me; and (C) coarse, Cse, size fractions.

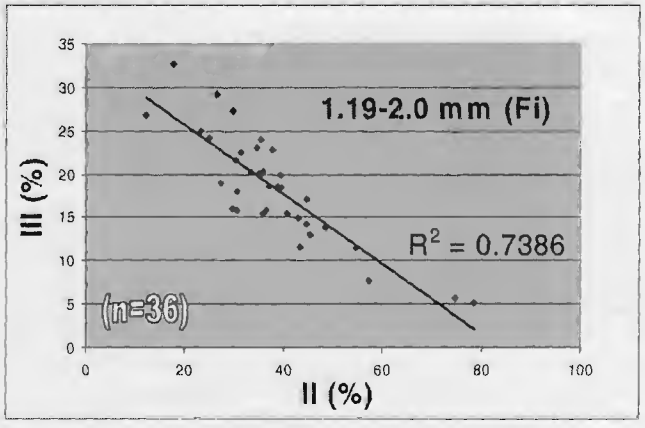

Figure 8. Scatter plots (region-wide, all samples, n = 36) showing inverse correlation between equant (II) and bladed (III) sphericity classes in the fine (Fi) size fraction.

the study area, *i.e.*, material in channels at high elevation nearest to the carbonate source terrain (n = 4) and at the lower extremity of the dispersal path adjacent to the Petit Lac shore (n = 3). Observations were made to detect possible relationships among roundness (B, C, D) and sphericity (I, II, III) and between them. In addition, roundness and sphericity were compared with three size parameters (percent sand, percent silt, and mean size).

(5) Roundness (B, C, D) and sphericity (I, II, III) data of the 28 samples collected along each of the six specific torrent paths were evaluated. The number of samples collected in the channels ranged from three in Nant Balmette to seven in Nant d'Oy. Based on comparisons between roundness and sphericity parameters derived from step 4 above (study of samples from extreme geographic positions), we selected those parameters (of B, C, D and of I, II, III) that recorded the potentially most useful relationships.

(6) Finally, using samples collected only along the six torrent paths (n = 28), sand and silt percentages and mean size were evaluated against distance from source terrain and elevation above msl. This served to test for possible influence of grain size on particle roundness and sphericity along transport dispersal paths.

OBSERVATIONS

Of the total number of grains counted, an average roundness of 0.6% was accounted for in class A, 11.8% in B, 54.9% in C, 31.9% in D, and 0.7% in E. The roundness data and percentages of the five classes in the Fi, Me, and Cse fractions

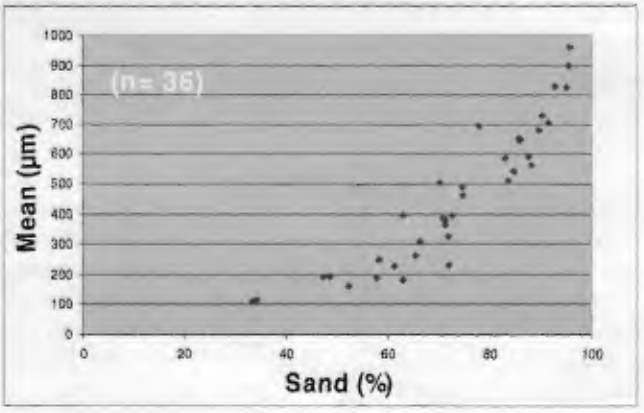

Figure 9. Scatter plot (region-wide, all samples, n = 36) showing positive correlation between percentage of sand and mean grain size.

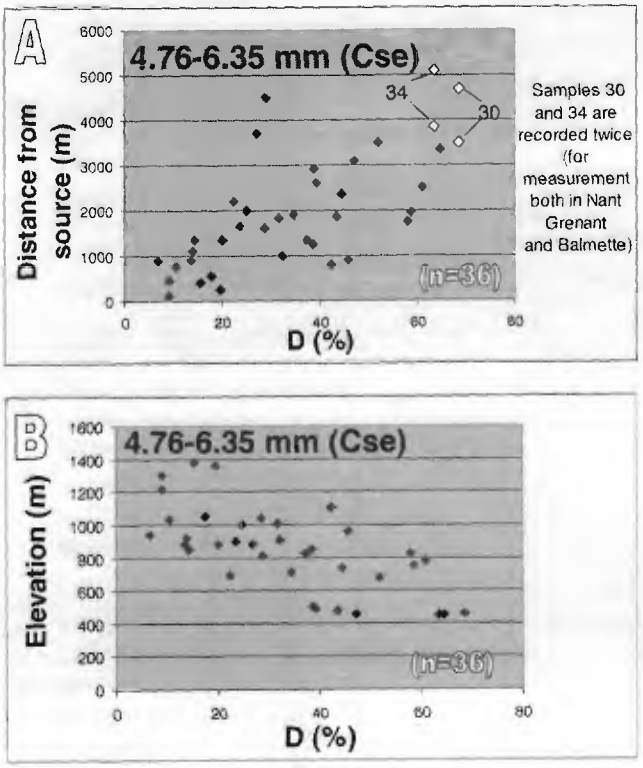

Figure 10. Scatter plots (region-wide, all samples, n = 36,) showing downslope trend of increased roundness (class D, in Cse fraction) as related to (A) distance from source (in meters) and (B) decrease in elevation (in meters) above mean sea level (msl).

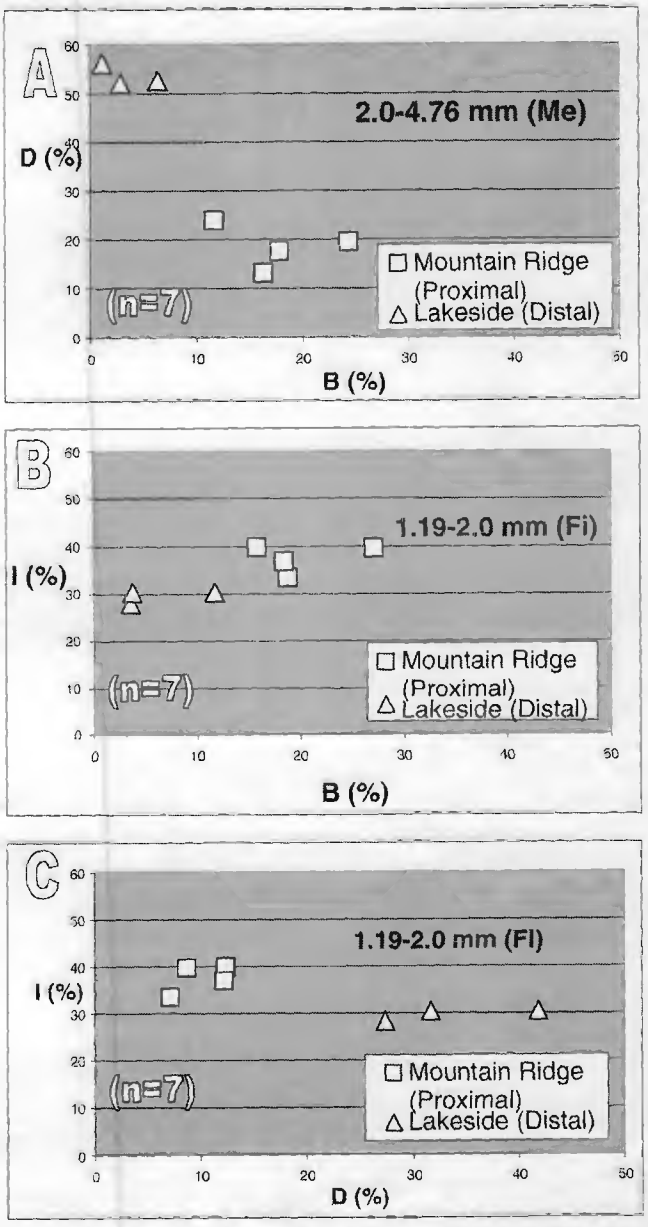

Figure 11. Scatter plots showing relationships of roundness and sphericity at extreme geographic localities (n = 7 samples). Note changes downslope from proximal sites at high elevations toward distal lakeside sites: (A) marked decrease in subangular (B) and increase in rounded (D) grains (medium [Me] fraction); (B) decrease in subangular (B) and slight decrease in tabular (I) grains (Fi fraction); and (C) marked increase in rounded (D) and slight decrease in tabular (I) grains (Fi fraction).

are shown in Table 1. The total percentage of subrounded class C is the most pronounced of the five. Moreover, the proportion of class C decreases, whereas those of classes A, B, and E increase in coarser-sized fractions.

Average sphericity abundances were calculated: 37.0% of class I; 33.7% of II; 20.7% of III; and 8.6% of IV. This sphericity data and percentages of the 4 classes in Fi, Me, and Cse fractions, are also shown in Table 1. The total percentage of tabular class (I) is the most prominent; proportions of bladed (III) class increase, whereas equant (II) and prolate (IV) classes decrease with coarsening of size fraction.

Data sets in the study were graphically compiled in a total of 337 scatter-point diagrams, and assessment of each was made by focusing on the degree of linear correlation of plotted data as computed by the R^2. It is of note that ~90% of the 337 graphic plots record random and statistically weak relationships; only about 30 of the diagrams indicate statistically modest to strong relationships. Roundness, sphericity, and grain size data sets are used to define, where possible, the following: (items 1 and 2) a broad perspective of diverse, region-wide trends; (3) variations occurring along dispersal paths related to distance from source terrains; (4) more specific variations at extreme geographic positions, in proximal high source terrains and at distal lakeshore elevations; (5) downslope trends along six distinct channel paths; and (6) possible downslope associations with grain size parameters.

(1) Roundness parameters in all samples (n = 36) in the study area indicate a general inverse correlation between subangular (B) and rounded (D) classes in Fi, Me, and Cse size fractions (Figures 7A–7C). Correlation is strongest in the Cse (R^2 value = 0.5549) fraction. Comparable but more modest correlations are recorded between subrounded (C) and rounded (D) classes in the three size fractions.

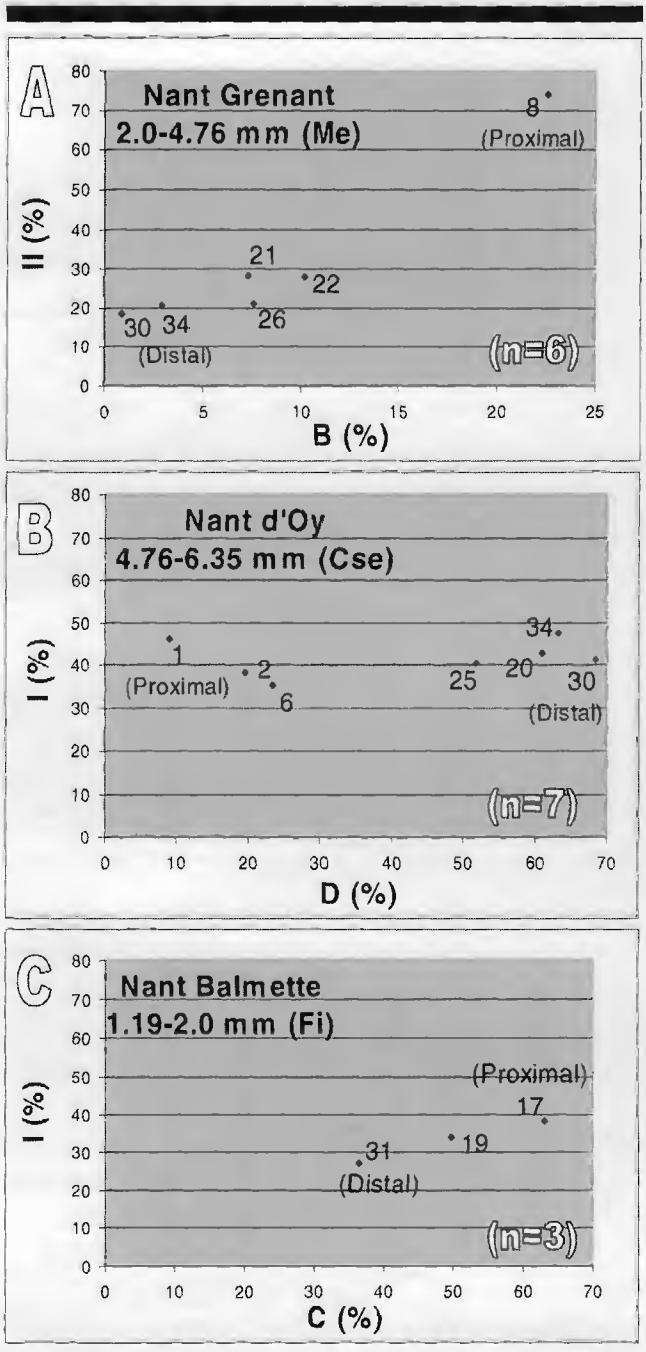

Figure 12. Downslope changes along dispersal paths in three channels, from proximal mountain source area to distal lake shore: (A) decrease in both subangular (B) and equant (II) grains in Nant Grenant (Me fraction); (B) increase of rounded (D) grains but no sphericity (tabular I) change in Nant d'Oy (Cse fraction); and (C) decrease in subrounded (C) and subtle decrease in tabular (I) particles in Nant Balmette (fine [Fi] fraction).

In all 36 samples, there is a strong inverse correlation of sphericity parameters between equant (II) and bladed (III) particles in the three size fractions; the relationship is strongest in the Fi fraction (R^2 value = 0.7386; Figure 8). A similar, but weaker, correlation is measured between equant (II) and tabular (I) grains. Regionally, there is also a direct correlation between percentage of sand and mean grain size (Figure 9), whereas proportions of sand and silt are inversely related, as are proportions of silt and mean size.

(2) Correlations were also determined among the three roundness *vs.* three sphericity classes on a region-wide basis (n = 36 samples). The only two trends observed are weak ones, *i.e.*, between equant (II) and angular (B) grains and between equant (II) and rounded (D) grains, particularly in the Cse fraction (R^2 value = 0.1623 and 0.1107, respectively). Regionally, angular grains show a subtle increase and rounded grains tend to decrease with larger proportions of equant particles. There are no significant trends among grain-size, sphericity, and roundness parameters.

(3) Region-wide relationships among distance from source and elevation, sphericity, and roundness were determined for the Fi, Me, and Cse fractions using all 36 samples. The clearest trends are revealed by D (rounded) particles that increase significantly, from <10% to more than 50%, downslope and away from the source as best-indicated by the coarser (Me, Cse) size fractions (Figures 10A and 10B). Inversely, proportions of B (angular) and C (subrounded) grains decrease downslope, particularly in coarser fractions. In marked contrast, no strong downslope trends are indicated by sphericity, and only a slight decrease of III (bladed) grains is observed in a distal direction. Moreover, there are subtle region-wide trends indicating a downslope decrease in percentage of sand and mean grain size and an increase in percentage of silt.

(4) Samples (n = 7) collected at extreme geographic positions (proximal at the base of the high cliffs and distal on the lakeshore) show an inverse relationship between rounded (D) and subangular (B) grains in the Fi and Me fractions (Figure 11A) and between rounded (D) and subrounded (C) particles in the Me and Cse fractions. No distinct proximal *vs.* distal sphericity relationships are observed. Correlations among roundness *vs.* sphericity data record more subtle relationships: between tabular (I) and subangular (B) grains in the Fi and Me fractions (Figure 11B) and between tabular (I) and rounded (D) grains in that same fractions (Figure 11C). Size parameters in the seven samples from geographically extreme localities show no distinct relationships among each other or with roundness and sphericity.

(5) Findings pertaining to roundness and sphericity in the 28 samples collected along the six torrent channel axes are summarized. Only those downslope trends that indicate some systematic change from proximal sites at higher elevations to more distal ones near and at the lakeshore are specified below:

- Nant Sec (downslope sample site sequence: 27, 24, 33, 35; length of dispersal path 3.2 km). Along this stream, only sediment in sample 27 at the site most proximal to the source terrain can be differentiated from that in the three lower samples. Sample 27 has slightly higher proportions of class B, C, I, and III particles and lower proportions of class D and II grains.
- Nant Graz (downslope sample site sequence: 9, 29 23, 32, 36; length of path 3.4 km). The most proximal sample 9 is the only one along the stream channel that can be differ-

entiated somewhat from the other four, more distal, samples. It is characterized by slightly higher proportions of classes C and II grains and lower proportions of class D particles.

- Nant Grenant (downslope sample site sequence: 8, 22, 21, 26, 30, 34; length of path 3.8 km). The most proximal sample 8 can be clearly differentiated from the other five, more distal ones. It has higher proportions of class B and II grains (Figure 12A) and lower proportions of class D, I, and III particles.
- Nant d'Oy (downslope sample site sequence: 1, 2, 6, 20, 25, 30, 34; length of path 5.1 km). The uppermost sample 1 has higher proportions of class B and C grains and lower proportions of D particles. The sequence of proximal samples 1, 2, and 6 can also be differentiated from the four lower, more distal samples: the proximal samples display higher proportions of class B grains and lower proportions of D particles (Figure 12B).
- Nant Balmette (downslope sample site sequence: 17, 19, 31; length of path 1.9 km). The three samples along this fluvial system record a series of consistent downslope trends. The most proximal sample, 17, is characterized by higher proportions of class C, I, and II (Figure 12C) and lower proportions of class B and D particles.
- Nant Montmin (downslope sample site sequence: 3, 10, 15, 13, 14; length of path examined 4.5 km). Proximal samples 3 and 10 can be differentiated from the three more distal ones at lower elevations. The two proximal sites are characterized by higher proportions of class B and III grains and lower proportions of class D particles.

(6) A survey of grain-size, downslope trends along the six specific channel dispersal paths toward the lake shore is also made using the 28 samples, from north to south:

- Nant Sec, a decrease in percent sand and mean grain size;
- Nant Graz, no consistent trends noted;
- Nant Grenant, an increase in percentage of sand and in mean grain size and decrease in percentage of silt;
- Nant d'Oy, an irregular decrease in percentage of sand and mean grain size toward the lower slope (between sample sites 1 to 25), and then below site 25 (elevation of less than 700 m at ~3.5 km from source), a marked increase toward the Angon fan-delta and lake shore (between samples 25–34; Figure 13);
- Nant Balmette, a decrease in percentage of sand and mean grain size and an increase in percentage of silt; and
- Nant Montmin, the two proximal samples comprise somewhat higher percent silt and lower percentage of sand and mean grain size with respect to particles at sites further downslope.

POORLY DEFINED TEXTURAL TRENDS

Region-wide Downslope Changes

Observations made in the L.A. study area record only several moderate- to well-defined region-wide downslope trends when taking into account the entire 36 sample database. Higher relative proportions of rounded (D) particles are associated with sediment characterized by lower amounts of both subangular (B) and subrounded (C) grains. Relative proportions of subangular (B) and subrounded (C) grains are generally greater at sites nearest high-relief source terrains and at midslope (Figure 2D and 2E); in contrast, proportions of rounded (D) particles increase downslope within several kilometers, *i.e.,* toward distal sites at some midslope elevations and near the lake margin (Figure 3D). As to sphericity, sediment with higher amounts of equant (II) particles usually comprise smaller proportions of flattened particles, both bladed (III) and tabular (I). Region-wide sphericity changes, however, record only a slight downslope decrease in bladed (III) grains along the dispersal path. Correlations among roundness and sphericity classes are not distinct: noted are a weak positive correlation between subangular (B) and equant (II) grains and an inverse one between rounded (D) and equant (II) particles. There is also a positive correlation between sand percentage and mean size and an inverse correlation between these two parameters and percentage of silt.

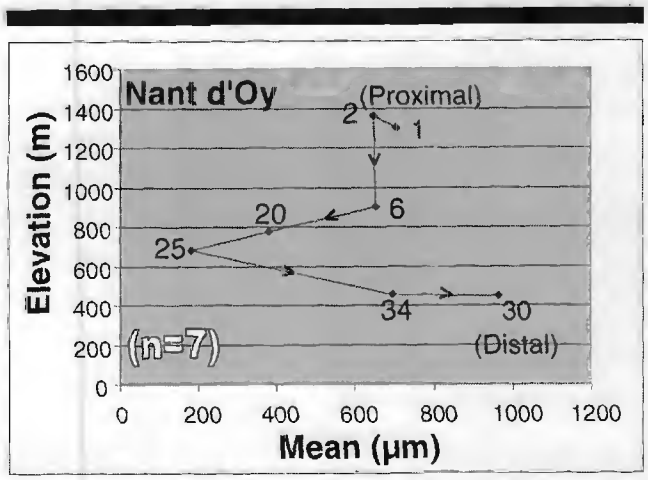

Figure 13. Scheme showing poorly defined, inconsistent grain size trend in Nant d'Oy. Mean size decreases irregularly to lower slope (site 25) and then increases toward the Angon fan-delta at lake margin (sites 30 and 34). The increase in mean size downslope records effects of valley wall influx and, on the distal base-of-slope fan-delta, human-induced effects. Discussion in text.

Grain texture measurements of samples collected at extreme geographic positions (adjacent to source terrains *vs.* distal sites at the base of slope and at the lake shore) are generally comparable to the above-recorded region-wide trends. Most apparent are higher proportions of subangular (B), subrounded (C), and tabular (I) grains at proximal sites near high source terrains, whereas rounded (D) particles prevail at lower elevations near and at the lake margin.

Thus, the region-wide survey indicates that as carbonate moves a short distance downslope, there is a general overall increase in rounding, decrease in grain size, and a poorly defined change in sphericity. These findings suggest that samples located only a few kilometers from where sediment originates record effects of abrasion and grain breakage during the initial transport stages (*cf.* KRUMBEIN, 1941). However, unlike findings in some laboratory experiments, there is only a weak correlation between rounding and grain size, with no

marked increase of particle rounding in coarser size fractions. It is recalled that other studies in various settings have shown that sphericity characteristics have less environmental sensitivity than roundness and that the two parameters do not necessarily evolve at the same rate along the transport path. Comparison of present study findings with other investigations (references cited earlier) indicate that sphericity is more poorly developed downslope than expected.

Inconsistent Trends Along Specific Channels

This study also records highly irregular and, for the most part, poorly developed downslope trends recorded by the samples (n = 28) collected in the six fluvial channels. Several observations similar to the region-wide pattern are noted: locally higher proportions of subangular (B) and subrounded (C) grains at sites most proximal to high source areas and increased relative amounts of rounded (D) particles near the lake. There is a generally inconsistent sample-to-sample pattern of grain roundness and sphericity along the mid- and lower courses of the six channels. For example, tabular (I) and bladed (III) particles prevail near some high-elevation source areas (Figure 2D), whereas in others, equant (II) are more common. Relative proportions of I, II, and III vary irregularly downslope from sample site to sample site along the six dispersal paths. Also noted are erratic patterns among percentage of sand, percentage of silt, and mean grain size, on one hand, and distance downslope from source areas and elevation on the other (Figure 13). Analyses reveal the following inconsistent patterns: proximal up-slope samples in three channels (Nant Sec, d'Oy, Balmette) comprise larger proportions of sand and larger mean size; samples in the upper part of two other torrents (Nant Grenant and Montmin) record a higher percentage of silt; and size parameters in a sixth, Nant Graz, revealed no downslope transport path patterns.

VALLEY WALL SEDIMENT INFLUX AND OTHER FACTORS

It has been shown that limestone fragments can decrease in size by mechanical attrition in as little as a few hundred meters of movement (KRUMBEIN and GRIFFITH, 1938). Yet, trends of grain roundness, sphericity, and size along the six channel dispersal paths between source terrains and lake shore are either poorly developed or highly irregular and do not clearly reveal systematic and progressive downslope effects of abrasion. It is not likely that these observations result from an irregular sampling spacing pattern alone. Major factors that are normally considered to determine particle shape include distance of travel and intensity of transport agent. Also significant are attributes of the rock material at source rock exposures that influence grain shape, such as composition, hardness, and inherited parting. The initial shape of carbonate fragments giving rise to sediment in the study area is primarily angular and flat (Figure 2D), either tabular (I) or bladed (III). Further fracture by impact (Figures 6I–6L) would prevail in the case of carbonate fragments characterized by natural zones of weakness, including fissility (Figures 6A, 6E, and 6H) and the presence of veins (Figure 6G). Investigations by other workers have also indicated that abrasion of sand and granule-sized particles is substantially increased by the presence of coarse material (pebbles, cobbles, boulders) that fracture smaller grains during transport (*cf.* MARSHALL, 1927). The abrasive action of sand blasting, as finer particles move over and bypass carbonate pebbles, also modifies the shape and size of larger clasts. In sum, there is an extensive suite of interactive factors that collectively alter grain texture along the short initial downslope transport path toward the lake.

The discontinuous and poorly developed trends of particle texture in each of the six channels should also be associated with topographically related factors. Channel axes on the mountain slopes are highly variable, with suddenly changing paths, widths, gradients, and flow volumes. These are associated with yet another factor that previously has not received sufficient attention: the influx of sediment derived laterally along the channel path from the outcrop exposures and scree deposits that form steep valley walls that contain the restricted and incised channels (Figures 2F and 4A–4C). This lateral influx results from rock-fall and mass-flow (debris flow) processes, sometimes triggered by precipitation that periodically displace mechanically unstable deposits of fine to very coarse material from cliffs and mountain flanks, down valley walls, and into the channels. This material comprises reworked Quaternary sediment and fresh-to-weathered Mesozoic rock debris derived from midslope exposures (Figures 2F, 4D, and 4E). The local input of this material provides an episodic influx of new carbonate particles with different textural characteristics into each of the fluvial systems, thus inducing the marked variable textural changes in grain roundness, sphericity, and size along transport paths. This irregular introduction of broken material of highly variable size (Figures 4D and 4E), much of it sharp-edged and angular (Figured 2E and 3F), largely precludes systematic development of well-defined changes in grain roundness, sphericity, and size away from the source terrains.

CONCLUSIONS

Previous studies of fluvial systems have identified the first few kilometers of downstream sediment transport as ones where the greatest changes in roundness, sphericity, and size occur. Most of these earlier analyses have indicated that there tends to be a progressive change during this initial phase of sediment dispersal, such as systematic increased rounding and decreased size. Region-wide analyses in the L.A. study area also record some alteration, but generally only moderately to poorly developed grain roundness and size, along the short dispersal distance from source terrains. Moreover, analyses of particle parameters in specific channels of this proximal L.A. transport sector indicate discontinuous downslope trends along the short, high-gradient channel segments where high-energy conditions, rapid wear, and attrition of particles are normally expected. The highly variable particle-texture trends in this dissected, high-relief Alpine terrain are largely caused by laterally introduced sediment on the steep valley walls that confine the channels. This local and episodic carbonate influx along the dispersal path alters the otherwise expected progressive downslope increase

in grain roundness, sphericity change, and decrease in grain size.

It is generally assumed that rapid rate of particle breakage and abrasion during initial sediment transport in a proximal fluvial environment gives rise to a set of grain roundness, sphericity, and size characteristics that provide a fairly distinct sediment texture baseline. The textural attributes acquired in proximal transport sectors serve as a means to predict further changes of sediment grains, usually gradual, as they are moved farther away from their source terrains. Definition of the highly irregular particle texture patterns in topographically complex and high-energy proximal fluvial settings is needed to more realistically interpret the depositional history of sediment in fluvial-to-coastal systems such as those in the Annecy study area.

ACKNOWLEDGMENTS

We thank Mr. T.F. Jorstad, National Museum of Natural History (NMNH), and Ms. E. Landau, San Diego State University, for their valuable technical assistance and support with this study. This manuscript was kindly reviewed by T.F. Jorstad and N.A. Ellis.

LITERATURE CITED

CURRAY, J.R. and GRIFFITHS, J.C., 1955. Sphericity and roundness of quartz grains in sediments. *Bulletin of the Geological Society of America,* 66, 1075–1096.

DOUDOUX, B.; BARFETY, J.C.; CARFANTAN, J.C.; TARDY, M., and NICOUD, G., 1992. *Notice Explicative de la Feuille Annecy-Ugine à 1: 50000.* Orléans, France: Bureau de Recherches Géologiques et Minières, 62 p.

FRIEDMAN, G.M. and SANDERS, J.E., 1978. *Principles of Sedimentology.* New York: John Wiley & Sons, 792 p.

GRIFFITHS, J.C., 1967. *Scientific Methods in Analysis of Sediments.* New York: McGraw-Hill Book Co., 508 p.

INSTITUT GEOGRAPHIQUE NATIONAL, 2003. *Carte de Randonnée, Lac d'Annecy.* Topographic map, Paris: Edition IGF, scale 1 cm = 250 m, sheet number 3431 OT.

KRUMBEIN, W.C., 1941. Measurement and geologic significance of shape and roundness of sedimentary particles. *Journal of Sedimentary Petrology,* 11, 64–72.

KRUMBEIN, W.C. and GRIFFITH, J.S., 1938. Beach environment in Little Sister Bay, Wisconsin. *Bulletin of the Geological Society of America,* 49, 629–652.

KRUMBEIN, W.C. and PETTIJOHN, F.J., 1938. *Manual of Sedimentary Petrography.* New York: Appleton-Century-Crofts, 549 p.

KUENEN, P.H., 1964. Experimental abrasion, 6: surf action. *Sedimentology,* 3(1), 29–43.

MARSHALL, P.E., 1929. Beach gravels and sands. *Transactions and Proceedings of the New Zealand Institute,* 60, 324–365.

NICOUD, G. and MANALT, F., 2001. The lacustrine depression at Annecy (France), geological setting and Quaternary evolution. *Journal of Paleolimnology,* 25, 137–147.

OLDFIELD, F. and BERTHIER, F., 2001. Lac d'Annecy (Special Issue). *Journal of Paleolimnology,* 25(2), 133–269.

PETTIJOHN, F.J., 1957. *Sedimentary Rocks,* 2nd edition. New York: Harper & Row, 718 p.

PETTIJOHN, F.J.; POTTER, P.E., and SIEVER, R., 1972. *Sand and Sandstone.* New York: Springer-Verlag, 618 p.

STANLEY, J.-D. and JORSTAD, T.F., 2004. Direct sediment dispersal from mountain to shore, with bypassing via three human-modified channel systems to Lake Annecy, SE France. *Journal of Coastal Research,* 20, 958–969.

WADELL, H.A., 1932. Volume, shape, and roundness of rock particles. *Journal of Geology,* 40(5), 443–451.